Structure and Partial Stereochemical Assignments for Maitotoxin, the Most Toxic and Largest Natural Non-Biopolymer[1]

Michio Murata,*,†,‖ Hideo Naoki,‡ Shigeki Matsunaga,§ Masayuki Satake,† and Takeshi Yasumoto*,†

Contribution from the Faculty of Agriculture, Tohoku University, Tsutsumidori-Amamiya, Aoba-ku, Sendai 981, Japan, Suntory Institute for Bioorganic Research, 1-1 Wakayamadai Shimamoto-cho, Osaka 618, Japan, and Faculty of Agriculture, The University of Tokyo, Yayoi, Bunkyo-ku, Tokyo 113, Japan

Received February 7, 1994®

Abstract: Maitotoxin (MTX), with a molecular weight of 3422, was first discovered as one of the toxins responsible for ciguatera, a seafood poisoning caused by coral reef fish. For this study MTX was isolated from cultured cells of the ciguatera-causative dinoflagellate *Gambierdiscus toxicus* and was subjected to extensive 2D NMR measurements. A large portion of the structure was shown to be a brevetoxin-type polyether. Precise structural assignments were, however, unsuccessful, chiefly due to extensive overlapping of ^1H and ^{13}C NMR signals even in the 2D spectra. MTX was treated with $NaIO_4$ followed by reduction with $NaBH_4$, resulting in cleavage of the molecule into two major parts, fragments A and B, together with a small C_9 fragment. Fragments A and B had molecular weights of 964 and 2328. Their structures were elucidated by extensive 2D NMR and collisionally activated dissociation (CAD) MS/MS experiments. Reassembling the three fragments led to the complete structure of MTX ($C_{164}H_{256}O_{68}S_2Na_2$), encompassing two sulfate esters, 28 hydroxyls, and 32 ether rings. Relative stereostructure was partly assigned and comprised trans-fused polycyclic ethers except for rings L/M and N/O that are cis-fused. The stereochemistry of the acyclic parts, C5-C14, C36-C37, C64-C66, and C135-C139, remains to be determined.

Ciguatera is a form of seafood poisoning caused by ingestion of coral reef fish. The poisoning occurs widely over the Pacific Ocean and in the Caribbean Sea, posing a serious threat to public health and the fishing industry. The annual number of patients has been estimated to be around 20 000, making it one of the most widespread poisonings caused by natural toxins.

Maitotoxin (MTX, **1** in Figure 1) was first discovered from the surgeonfish *Ctenochaetus striatus* as one of the causative toxins of ciguatera[2,3] and was named after the Tahitian fish *maito*. The toxins accumulated in herbivorous fish are diverse. Ciguatoxins,[3] maitotoxin, palytoxin,[4] and other toxins produced by algae[5] are thought to be implicated in the poisoning, while poisoning by carnivorous fish is attributable mostly to ciguatoxins. Subsequently, MTX and ciguatoxins were found to originate in the epiphytic dinoflagellate *Gambierdiscus toxicus*.[6]

Among natural products, MTX has attracted much attention, since it has the largest molecular weight (3422 Da nominal mass) of any natural product known to date aside from biopolymers like proteins or polysaccharides.[7] Furthermore, its powerful bioactivity has stimulated the interest of pharmacologists and biochemists. In lethal potency against mice, MTX is one of the most potent toxins, exceeded only by the lethality of a few proteins. Additionally, the toxin possesses multiple activities, such as hormone stimulation, neurotransmitter release, activation of phosphoinositide degradation, and potentiation of protein kinase, all of which appear to be linked to elevation of the intracellular Ca^{2+} concentration.[8] Thus the toxin serves as a versatile tool for studies on cellular events associated with Ca^{2+} flux.

In two previous communications and a review,[1] we have briefly reported that the planar structure of MTX comprises a C_{142} carbon chain encompassing 32 ether rings, 28 hydroxyl groups, and two sulfate esters. In this paper, we report the structure of MTX including partial stereochemical assignments.

Results and Discussion

Chemical Properties and Toxicity of Maitotoxin. MTX for this study was isolated from cultured cells of *G. toxicus*. The physicochemical properties of MTX were published in a previous paper.[7] An elemental analysis of an MTX sample that was passed once through an HPLC column (see the Experimental Section) suggested the presence of one nitrogen atom (C 53.3%, H 7.65%, and N 0.48%), whereas the proposed structure bore no nitrogen. After treatment with a cation exchanger,[9] no nitrogen could be detected in MTX by elemental analysis, suggesting that the earlier nitrogen content was derived from a countercation of one of the sulfate esters and had been retained during purification. After repeated chromatography by HPLC, the signals corresponding to the counterion disappeared or were much decreased in the ^1H NMR spectrum of MTX. From the ^1H and ^{13}C NMR resonances,[10] the countercation appeared to be triethylammonium.

† Tohoku University.
‡ Suntory Institute.
§ The University of Tokyo.
‖ Present address: Department of Chemistry, The University of Tokyo, Hongo, Bunkyo-ku, Tokyo 113, Japan.

® Abstract published in *Advance ACS Abstracts*, July 1, 1994.

(1) Preliminary reports of the planar structure of maitotoxin appeared in the following: (a) *J. Am. Chem. Soc.* **1992**, *114*, 6594-6596. (b) *J. Am. Chem. Soc.* **1993**, *115*, 2060-2062. (c) *Chem. Rev.* **1993**, *93*, 1897-1909.

(2) Yasumoto, T.; Bagnis, R.; Vernoux, J. P. *Bull. Jpn. Soc. Sci. Fish.* **1976**, *42*, 359-365.

(3) (a) Murata, M.; Legrand, A.-M.; Ishibashi, Y.; Yasumoto, T. *J. Am. Chem. Soc.* **1989**, *111*, 8927-8931. (b) Murata, M.; Legrand, A.-M.; Ishibashi, Y.; Fukui, M.; Yasumoto, T. *J. Am. Chem. Soc.* **1990**, *112*, 4380-4386.

(4) (a) Moore, R. E.; Bartolini, G. *J. Am. Chem. Soc.* **1981**, *103*, 2491. (b) Uemura, D.; Ueda, K.; Hirata, Y. *Tetrahedron Lett.* **1981**, *22*, 2781-2784. (c) Fukui, M.; Murata, M.; Inoue, A.; Gawel, M.; Yasumoto, T. *Toxicon* **1987**, *25*, 1121-1124.

(5) Yasumoto, T.; Murata, M. *Chem. Rev.* **1993**, *93*, 1897-1909.

(6) Yasumoto, T.; Nakajima, I.; Bagnis, R.; Adachi, R. *Bull. Jpn. Soc. Sci. Fish.* **1977**, *43*, 1021-1026.

(7) Yokoyama, A.; Murata, M.; Oshima, Y.; Iwashita, T.; Yasumoto, T. *J. Biochem.* **1988**, *104*, 184-187.

(8) Takahashi, M.; Ohizumi, Y.; Yasumoto, T. *J. Biol. Chem.* **1982**, *257*, 7287-7289.

(9) To replace the counterions, MTX (3 mg) was dissolved in 1 mL of H_2O and treated with 50 mg of Dowex 50 (Na^+-form, Organo) for 12 h with stirring.

0002-7863/94/1516-7098$04.50/0

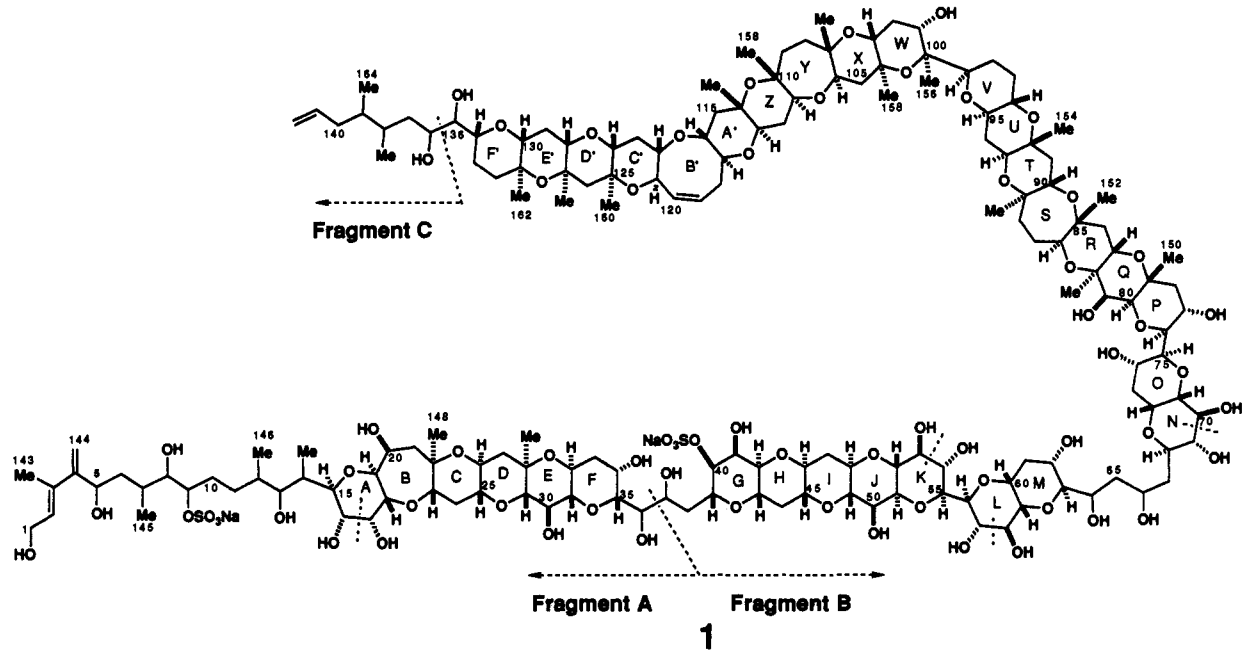

1

Figure 1. Structure of maitotoxin. Dashed lines denote cleavage sites by periodate degradation. Diastereomeric relations among rings A–F, G–M, and N–F′ remain unknown.

In this study, however, most of the specimens purified as described below contained hardly any ammonium ion, and we represent the structure (**1**) as a disodium salt. Thus the presence of nitrogen covalently bonded to MTX as previously suggested[7] was clearly ruled out.[11]

The lethal potency reported in the previous paper[7] (130 ng/kg) has been revised to an LD_{50} value of 50 ng/kg against male mice of a ddY strain, weighing 16–20 g, by intraperitoneal injection.[12] MTX was reported to have extremely potent cytotoxicity against various cell lines and tissue preparations. The cytotoxicity and other pharmacological activities of MTX have been reviewed.[13]

Spectral Measurements of Maitotoxin. A UV absorption maximum at 230 nm suggested the presence of a conjugated diene system.[7] The IR spectrum lacked C=O bands at 1600–1800 cm^{-1}, implying the absence of carbonyl functionalities.[7]

The negative ion FAB mass spectrum revealed a weak peak due to a molecular ion approximately at *m/z* 3400, in addition to a prominent peak at about *m/z* 3300, presumably generated by a loss of sodium sulfonate from the molecular ion. The fragment lost ($NaSO_3$–H, *m/z* 102) in the negative ion FABMS is characteristic of compounds possessing two or more sulfate esters or one sulfate plus an additional anionic functionality; in either case, a negative charge still remains after liberation of a sulfonate group.[14] It has therefore been suggested that MTX possesses two sulfate groups. These MS data have disclosed the molecular weight of MTX to be 3421–3423 as the nominal mass of the disodium salt.

The ^1H NMR spectrum of MTX showed five methyl doublets, 16 methyl singlets (including an olefinic methyl), and eight olefinic protons in addition to a great number of methylenes at δ 1.4–2.8 and oxygenated methines at δ 2.9–4.8 (Figure 2). A total of 160–165 resonances were observed in the ^{13}C NMR spectrum. Table 1 represents the number of carbons according to the degree of protonation estimated from the 1D and 2D NMR data of ^1H-decoupled and DEPT(135°)–^{13}C NMR spectra, ^{13}C-observed H–C COSY, and ^1H-observed HMQC (although the exact numbers presented in Table 1 were not determined until the full structural elucidation). The degree of unsaturation derived from the numbers of carbons and hydrogens implied the presence of more than 30 rings in MTX.

The number of the singlet methyls plus one exomethylene was equal to the number of the quaternary carbons (Table 1). The carbon atoms except the olefinic ones therefore bear a singlet methyl and an oxygen atom. Furthermore, the number of methines in the C–C region (5, see Table 1) agreed with that of doublet methyls; two olefinic quaternary carbons were assignable to those adjacent to an exomethylene and a vinyl methyl. These data suggested that all 22 carbons substituted by three carbon atoms were connected to the C_1-branching groups (21 methyls and an exomethylene at C4). Aside from these C_1 groups, there were only two carbons linked to a single carbon, which were an exovinyl group (C142) at δ 115.9 and a hydroxy methyl (C1) at δ 59.4. All the others were substituted by two carbons as part of a linear carbon chain. These facts revealed that the skeleton of MTX basically consisted of a linear 142-carbon chain substituted with 21 methyls and an exomethylene but lacking alicycles or longer carbon branches.

Extensive 2D NMR measurements were carried out with the intact MTX molecule, including conventional COSY, DQF-COSY, TOCSY, NOESY, heteroCOSY, HMBC experiments,[15] and new applications like HSQC or 2D HMQC-TOCSY by 600 MHz or 500 MHz instruments (most of these 2D spectra are available as supplementary material to the previous communications[1] as well as this paper). Among several interproton 2D experiments, those by phase-sensitive methods like DQF-COSY or TOCSY generated better information than did the absolute

(10) MTX bearing a nitrogen atom gave some ^1H and ^{13}C signals which were undetectable in the finally purified specimen or in that treated with the ion exchanger:[9] ^1H NMR δ 1.22 (7–9H, triplet, J = 7 Hz), 3.12 (5–6H, quartet, J = 7 Hz); ^{13}C NMR (CD_3OD/D_2O (1:1)) δ 9.0, 47.5. These chemical shifts agreed completely with those of triethylammonium (as a *p*-toluenesulfonate salt).

(11) The presence of nitrogen was suggested by a positive Dragendorff's test.[7] Even after replacing a counterion of MTX with sodium by means of ion exchange,[9] it was still positive to the test. One of the brevetoxins (PbTx-3, Wako Pure Chemical), which lacks a nitrogenous functionality, was found to be positive to the test, suggesting that polyether compounds belonging to the brevetoxin type might react with Dragendorff's reagent despite lack of nitrogenous groups.

(12) Toxicity of MTX seems to depend upon various conditions such as mice strain, purity of the sample, nature of the salt, and sample preparation; specifically, pure MTX does not dissolve well in H_2O and tends to adhere to the surface of glass or plastics.

(13) Gusovsky, F.; Daly, J. W. *Biochem. Pharmacol.* **1990**, *39*, 1633–1639.

(14) Kushi, Y.; Handa, S.; Ishizuka, I. *J. Biochem. (Tokyo)* **1985**, *97*, 419–428.

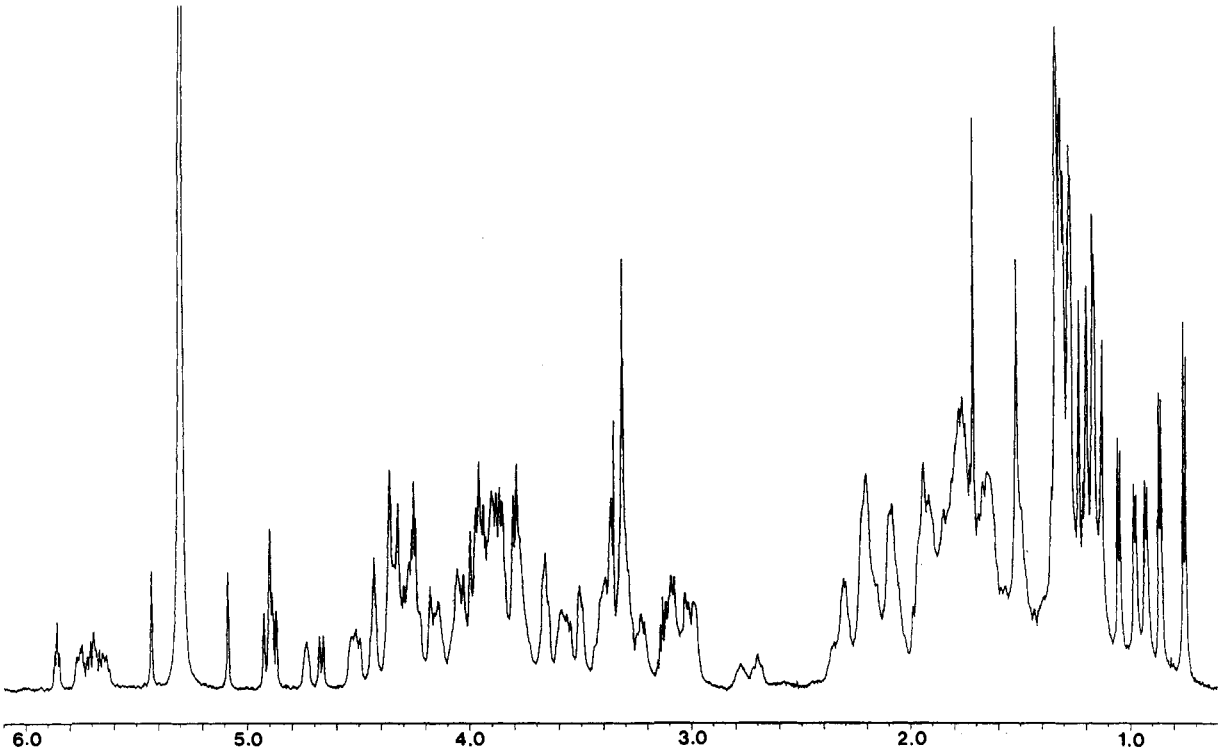

Figure 2. ^1H NMR spectrum of maitotoxin (**1**). (The spectrum was taken in C_5D_5N/CD_3OD (1:1) at 600 MHz.)

Table 1. Interpretation of ^{13}C NMR Spectra of Maitotoxin (**1**)

carbon species	CH_3	CH_2	CH	C	total
C=C (δ 110.8–154.8)	0	2	4	2	8
C—O (δ 59.4–87.7)	0	1	78	15	94
C—C (δ 10.6–53.2)	21	36	5	0	62
carbon	21	39	87	17	164
hydrogen (OH:28)	63	78	87	0	256

spectra, like conventional ^1H–^1H COSY. The reason was that ^1H NMR signals of MTX became broad mainly due to short T2 and the resonances with fast decaying FID were mostly lost after convolution by a window function used in the absolute mode.

Judging from NOEs and interproton coupling constants[16] shown in the 2D spectra, we deduced that most of the polycyclic ethers of MTX were trans–cisoid fused as was the case with other brevetoxin-type compounds.[17] This stereostructure caused ^1H NMR signals to show characteristic interactions such as strong NOEs between angular protons at 1,3-diaxial positions and large coupling constants[16] of 1,2-antiperiplanar protons. Some of the 2D NMR data could therefore be successfully interpreted and resulted in elucidation of partial structures as described in the following sections. However, overlapping of both ^{13}C and ^1H NMR signals hampered precise structural assignments, particularly for the central part of the molecule, where a great number of cross peaks extensively overlapped due to repeated similar structural moieties.

Chemical Degradation of Maitotoxin. In order to reduce the size of the molecule, several degradation reactions were carried out, e.g. periodate oxidation, ozonolysis, and acidic or basic hydrolysis. Upon ozonolysis, which has frequently been used for large natural products such as, for example, palytoxin,[4] MTX produces no structurally informative fragments since, of four C=C bonds, three are terminal parts of the molecule and one is in ring B′. Periodate degradation did work and resulted in cleavage of six vicinal diols C16/C17, C36/C37, C53/C54, C57/C58, C69/C70, and C135/C136 (dashed lines in Figure 1): those at C36/C37 and C135/C136 split the molecule into three parts. Oxidation of MTX (8.1 mg) with $NaIO_4$ followed by $NaBH_4$ reduction yielded fragments A (**2**, 1.6 mg) and B (**3**, 5.1 mg), which were separable by HPLC. Fragment C was not recovered, probably because of its low molecular weight and hence a small amount of product. Fragments B + C (C37–C142) were found in the reaction mixture as a minor product (5–10%), suggesting that the 1,2-diol at C135/C136 was less reactive.

Planar Structures of Fragments A and C. Fragment A (**2**) showed an $(M-Na)^-$ peak at m/z 941 in the FABMS. The proton connectivity of **2** was elucidated by usual 2D NMR methods like ^1H–^1H COSY or NOESY (Figure 3), while interrupted by two quaternary carbons (C22 and C28) and an acyclic ether (C15–O–C19). The corresponding part of intact MTX could be reconstructed from the structure of fragment A. There were four hydroxyl methyls in the fragment, three of which must have been generated by the degradation. They were assigned to C16, C17, and C36 by comparing the NMR spectra of **2** and of intact MTX (Table 2 and Figure 4). The location of the other hydroxyl groups was determined by deuterium shifts observed for ^{13}C NMR signals[18] and by acetylation of **2** (Figure 4). A sulfate ester was substituted at C9 because no substantial change in the chemical shift was observed for H9 following acetylation. Connectivities

(15) $^{2,3}J_{C,H}$ correlations shown in Figures 3 and 5 were established on the basis of the HMBC spectra of MTX measured in CD_3CN/D_2O (1:1) or in C_5D_5N/CD_3OD (1:1) (see the supplementary material to this paper and the previous communication[1b]). ^{13}C NMR assignments of the quaternary carbons and their adjacent carbons are as follows (C_5D_5N/CD_3OD (1:1)): δ C21, 48.3; C22, 79.0; C23, 80.5; C27, 45.2; C28, 75.4; C29, 86.1; C78, 49.8; C79, 75.5; C80, 81.3; C81, 75.2; C82, 76.4; C83, 64.7; C84, 40.8; C85, 78.5; C86, 74.2; C88, 39.5; C89, 79.5; C90, 72.0; C91, 43.1; C92, 75.2; C93, 71.8; C99, 87.8; C100, 78.8; C103, 72.7; C104, 74.5; C105, 42.8; C106, 84.2; C107, 79.7; C108, 39.0; C109, 40.3; C110, 78.4; C111, 87.8; C113, 83.8; C114, 74.1; C115, 46.9; C124, 84.3; C125, 73.4; C126, 54.0; C127, 75.4; C128, 86.9; C130, 84.3; C131, 75.2; C132, 38.4.

(16) From the cross peaks in the DQF-COSY or the NOESY of **1**, $^3J_{H,H}$ of angular protons was deduced to be 9–10 Hz, as exemplified by those of H18/H19, H25/H26, H31/H32, H42/H43, H48/H49, H51/H52, H54/H55, H56/H57, H62/H63, H68/H69, H74/H75, H76/H77, H95/H96, H116/H117, and H121/H122.

(17) (a) Lin, Y.-Y.; Risk, M.; Ray, S. M.; Van Engen, D.; Clardy, J. C.; Golik, J.; James, J. C.; Nakanishi, K. *J. Am. Chem. Soc.* **1981**, *103*, 6773–6775. (b) Shimizu, Y.; Chou, H.-N.; Bando, H.; VanDuyne, G.; Clardy, J. C. *J. Am. Chem. Soc.* **1986**, *108*, 514–515.

(18) Deuterium shifts in ^{13}C NMR signals were observed by measuring the ^1H-decoupled spectra (100 MHz) of **1** either in CD_3CN/D_2O or in CD_3CN/H_2O.

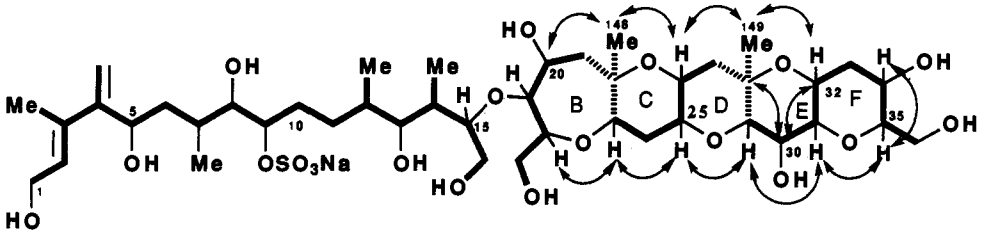

Figure 3. Fragment A (**2**) constructed by NMR data. Bold lines denote the connectivities elucidated on the basis of ^{1}H–^{1}H COSY data of **2** (see the supplementary material). Double-headed arrows indicate NOEs, which were mainly observed between angular protons and/or methyls and revealed from the NOESY of **1**. Broken lines represent $^3J_{C,H}$ detected as cross peaks from Me148 or Me149 in the HMBC spectrum of **1**.[15]

Table 2. ^{1}H NMR Assignments of Maitotoxin (**1**)[a]

postn	δ	postn	δ	postn	δ	postn	δ	postn	δ
1	4.23	34	4.43	69	3.27	101	3.85	132	1.73
	4.28	35	3.65	70	4.26	102	1.78		1.81
2	5.85	36	3.96	71	3.91		1.90	133	1.64
3		37	4.50	72	3.95	103	3.40		1.92
4		38	1.68	73	2.09	104		134	3.77
5	4.67		2.69		2.17	105	1.62	135	3.36
6	1.62	39	4.32	74	4.07		1.93	136	3.85
	2.09	40	4.32	75	3.94	106	3.58	137	1.25
7	2.35	41	4.90	76	3.90	107			1.76
8	3.93	42	3.02	77	4.37	108	1.77	138	1.85
9	4.73	43	3.75	78	1.70		1.94	139	1.39
10	1.81	44	1.35		2.22	109	1.77	140	1.73
	2.03		2.19	79			1.89		2.07
11	1.47	45	2.98	80	3.36	110		141	5.70
	2.14	46	2.98	81	3.99	111	3.43	142	4.88
12	1.66	47	1.50	82		112	1.76		4.91
13	3.50		2.30	83	4.25		1.88		
14	2.30	48	3.58	84	1.73	113	3.09	143	1.71
15	4.29	49	3.50		1.77	114		144	5.08
16	3.65	50	4.04	85		115	1.43		5.42
17	4.36	51	3.79	86	3.77		2.09	145	1.04
18	3.90	52	3.88[b]	87	1.63	116	3.66	146	0.98
19	3.80	53	3.77		1.93	117	3.40	147	0.93
20	4.18	54	3.87[b]	88	1.50	118	2.30	148	1.26
21	1.92	55	4.03		1.74		2.77	149	1.16
	2.22	56	4.24	89		119	5.64	150	1.51
22		57	3.95	90	3.82	120	5.75	151	1.12
23	4.43	58	4.35	91	1.63	121	4.35	152	1.31
24	1.71	59	3.88		1.77	122	3.33	153	1.31
	2.19	60	4.14	92		123	1.65	154	1.19
25	3.03	61	2.14	93	3.30		2.09	155	1.33[c]
26	3.38		2.22	94	1.48	124	3.22	156	1.32[c]
27	1.48	62	4.02		1.80	125		157	1.28
	1.95	63	3.55	95	3.07	126	1.62	158	1.27
28		64	4.53	96	3.29		1.97	159	1.15
29	3.08	65	1.89	97	1.33	127		160	1.22
30	3.85		2.08		1.84	128	3.33	161	1.33
31	3.11	66	4.31	98	1.49	129	1.83	162	1.29
32	4.13	67	1.57		1.80		1.95	163	0.85
33	1.65		2.22	99	3.31	130	3.23	164	0.76
	2.21	68	3.95	100		131			

[a] Chemical shifts are measured in C_5D_5N/CD_3OD (1:1). CD_2HOD was taken as a standard peak at δ 3.310. [b] Assignments are interchangeable. [c] Assignments are interchangeable.

around quaternary carbons C22 and C28 were established by $^{2,3}J_{C,H}$ as seen in HMBC spectra of **1** (Figure 3). The mode of cyclization of ether rings B–F was deduced mainly on the basis of NOEs observed between angular protons and/or methyls (Figure 3, details will be discussed below).

Fragment C was lost during the HPLC separation. The corresponding part of MTX was determined to be 3,4-dimethyl-6-hepten-1-ol on the basis of data from DQF-COSY and TOCSY experiments obtained with intact MTX.

Planar Structure of Fragment B. Small pieces of the ^{1}H–^{1}H spin networks of fragment B (**3**) were clarified by conventional 2D NMR experiments (bold lines in Figure 5). These fragmental structures were separated by three acyclic ethers and 13 sp^3-quaternary carbons.

The fragments separated by quaternary carbons were assembled on the basis of the HMBC and NOESY data. The connectivities around these carbons could be established directly by cross peaks due to $^{2,3}J_{C,H}$ interactions that were shown in the HMBC spectra of **1** (Figure 5).[15] All of them were adjacent to a methyl group, which gave rise to an intense ^{1}H NMR signal, and thus could be selectively detected by ^{1}H-observed HMBC experiments. Most long-range $J_{C,H}$ interactions were evident in the spectrum, leading to sequencing of the fragments into a larger piece (C70–C135, Figure 5).

Locations of hydroxyl groups were determined by comparing the ^{1}H chemical shifts of **3** with those of its acetyl derivative. As shown in Figure 4, the ^{1}H NMR signals of acetoxy methines or methylenes were shifted downfield by 0.5–1.3 ppm and were neatly separated from those due to ether methines. Thus, simply by comparing their chemical shifts, one could determine whether a proton was adjacent to a carbon bearing acetoxy or ether. The position of one sulfate ester was at C40 as suggested by an acetylation experiment (Figure 4). CAD MS/MS supported it by a prominent ion peak at *m/z* 167 that was apparently derived from cleavage between C40 and C41 and between C39 and the ether oxygen of ring G (Figure 6c), indicating C40 to be the site for sulfate substitution.

For the fusion between rings H and I, the connectivity of C45/C46 could not be proven directly because the chemical shifts of H45 and H46 were very close. Connectivities other than C45/C46 were evident from DQF-COSY data. The ^{13}C chemical shifts of C44–C47 of **1** (δ in CD_3CN/D_2O (1:1) C44, 35.2; C45/C46, 77.0/77.1; C47, 36.4) were typical values for trans-fused tetrahydropyran rings as reported for yessotoxin,[19] which is another brevetoxin-type polyether found in association with shellfish poisoning. In the NOESY spectrum of **1**, NOEs were observed as cross peaks from the equivalent H45/H46 versus H42, H43, H44ax, H47ax, H48, and H49. These data indicated that H45 and H46 resided on the same tetrahydropyran ring with an antiperiplanar orientation. The structures of the other symmetric portions or repetitive units C58–C63 and C70–C75 were elucidated by use of intact MTX (**1**), since ^{13}C NMR assignments that were necessary for interpreting the ^{1}H NMR data were obtained only for MTX itself.

Despite all structural information accumulated through measurements of numerous 2D spectra, overlapping signals coupled with the presence of three acyclic ethers prevented us from unambiguous assignments of the structure of fragment B. Thus we had to resort to complementary experiments in order to confirm the structure.

We reported successful application of negative ion FAB CAD (collisionally activated dissociation) MS/MS for the structural verification of yessotoxin.[19] In the course of that study, it was demonstrated that the fused polycyclic ethers of yessotoxin gave rise to characteristic fragmentations, from which sizes of ether rings and/or substituents on rings could be deduced directly.[20]

(19) Murata, M.; Kumagai, M.; Lee, J.-S.; Yasumoto, T. *Tetrahedron Lett.* **1987**, *28*, 5869–5872.
(20) Naoki, H.; Murata, M.; Yasumoto, T. *Rapid Commun. Mass Spectrom.* **1993**, *7*, 179–182.

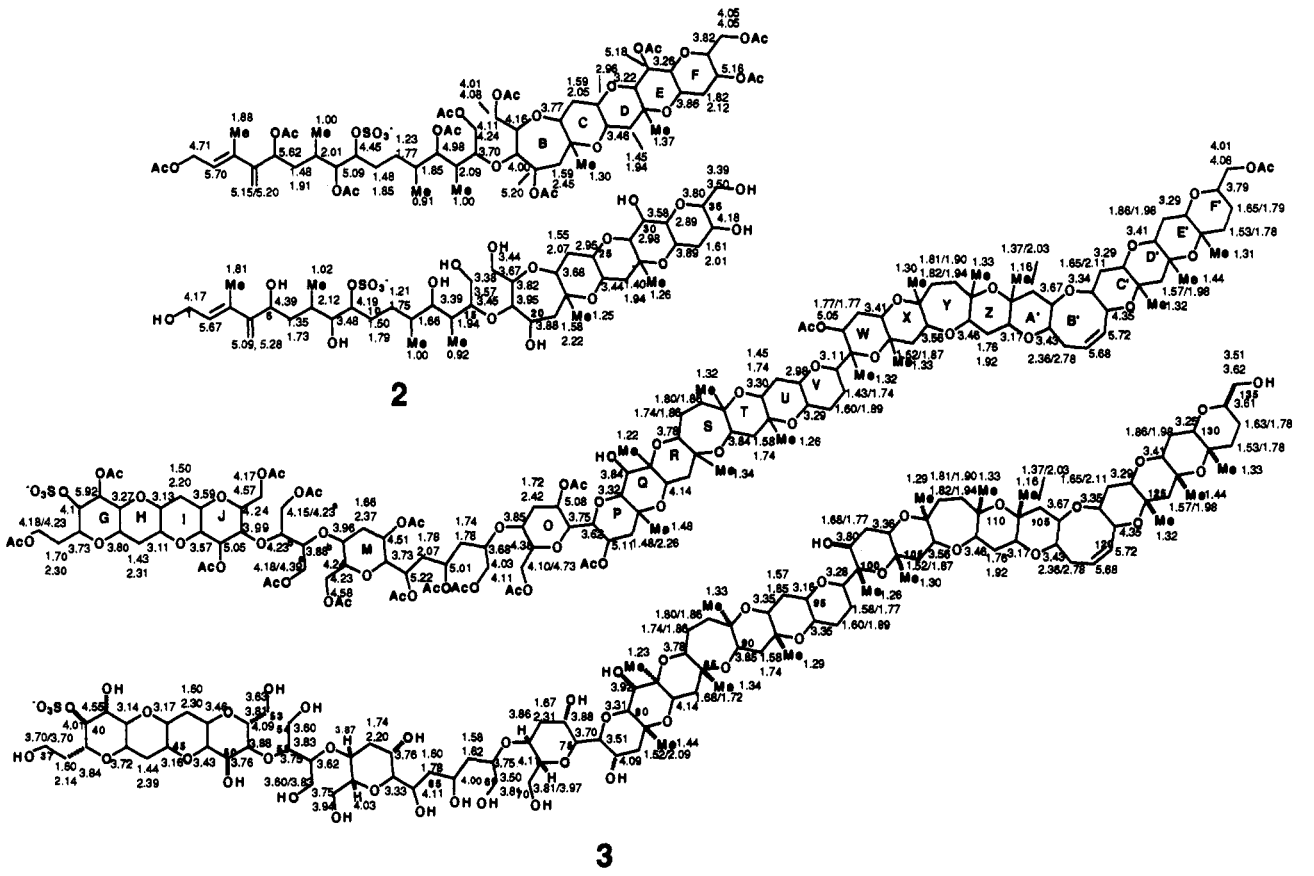

Figure 4. ^1H NMR assignments of fragment A (**2**), fragment B (**3**), and their acetyl derivatives. Chemical shifts are those in $(CD_3)_2SO$ for fragment A, in CD_3OD for its peracetate, and in CD_3OD for fragment B and its acetyl derivative. Superscripts a, b, and c denote that assignments are interchangeable.

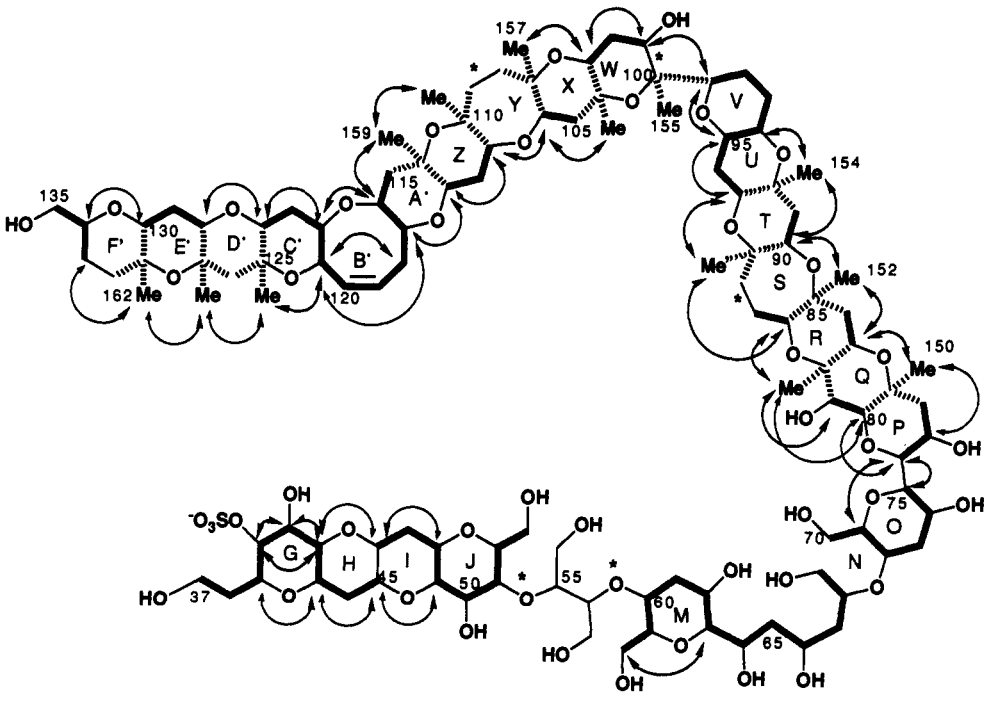

Figure 5. Fragment B (**3**) constructed mainly by NMR data. Bold lines denote connectivities elucidated on the basis of the ^1H–^1H COSY, DQF–COSY, or TOCSY data of **3**. Double-headed arrows indicate the NOEs mainly observed between angular protons and/or methyls shown in the NOESY of **3** or **1**. Broken lines depicted $^{2,3}J_{C,H}$ correlations from angular methyls shown in the HMBC spectrum of **1**.[15] *Connectivities were mainly elucidated on the basis of the MS/MS experiments.

Thus we chose MS/MS as a method complementary to NMR for verifying the structure.

Negative ion FABMS of fragment B revealed a molecular ion at m/z 2305 $(M-Na)^-$. Simulation of isotope distribution for composition $C_{112}H_{178}O_{47}S$ indicated that the ion at m/z 2305 corresponded solely to the mass composed of ^{12}C nuclei. A CAD MS/MS experiment carried out for this particular ion facilitated straightforward interpretation of the data because neither multiple peaks nor loss of sensitivity due to ^{13}C nuclei was shown in the spectrum (Figure 6). In addition to that, the sulfate ester near

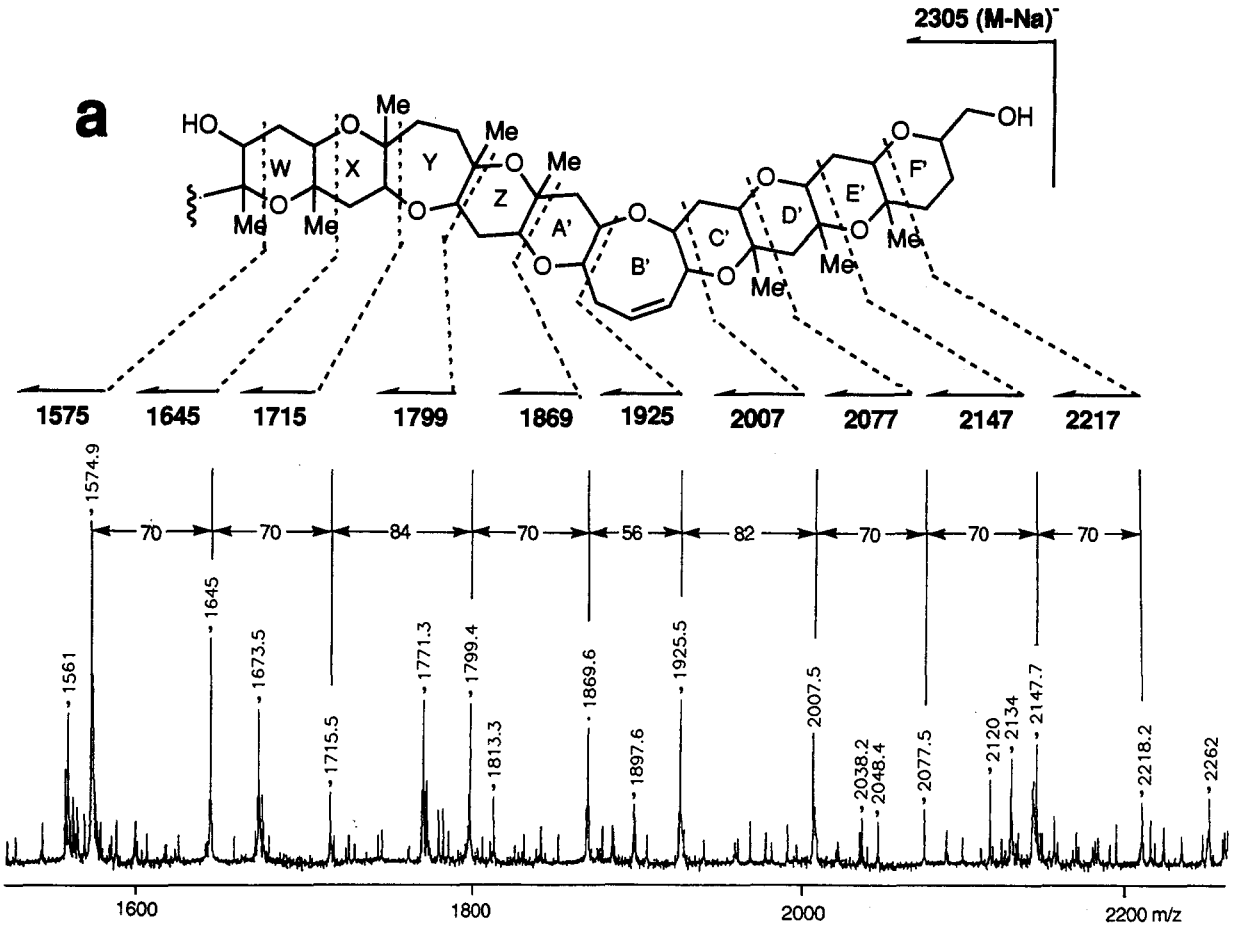
a
2305 (M-Na)⁻
HO
OH
Me
W
X
Y
Z
A'
B'
C'
D'
E'
F'
1575
1645
1715
1799
1869
1925
2007
2077
2147
2217
1574.9
70
70
84
70
56
82
70
70
70
1561
1645
1673.5
1715.5
1771.3
1799.4
1813.3
1869.6
1897.6
1925.5
2007.5
2038.2
2048.4
2077.5
2120
2134
2147.7
2218.2
2262
1600
1800
2000
2200 m/z

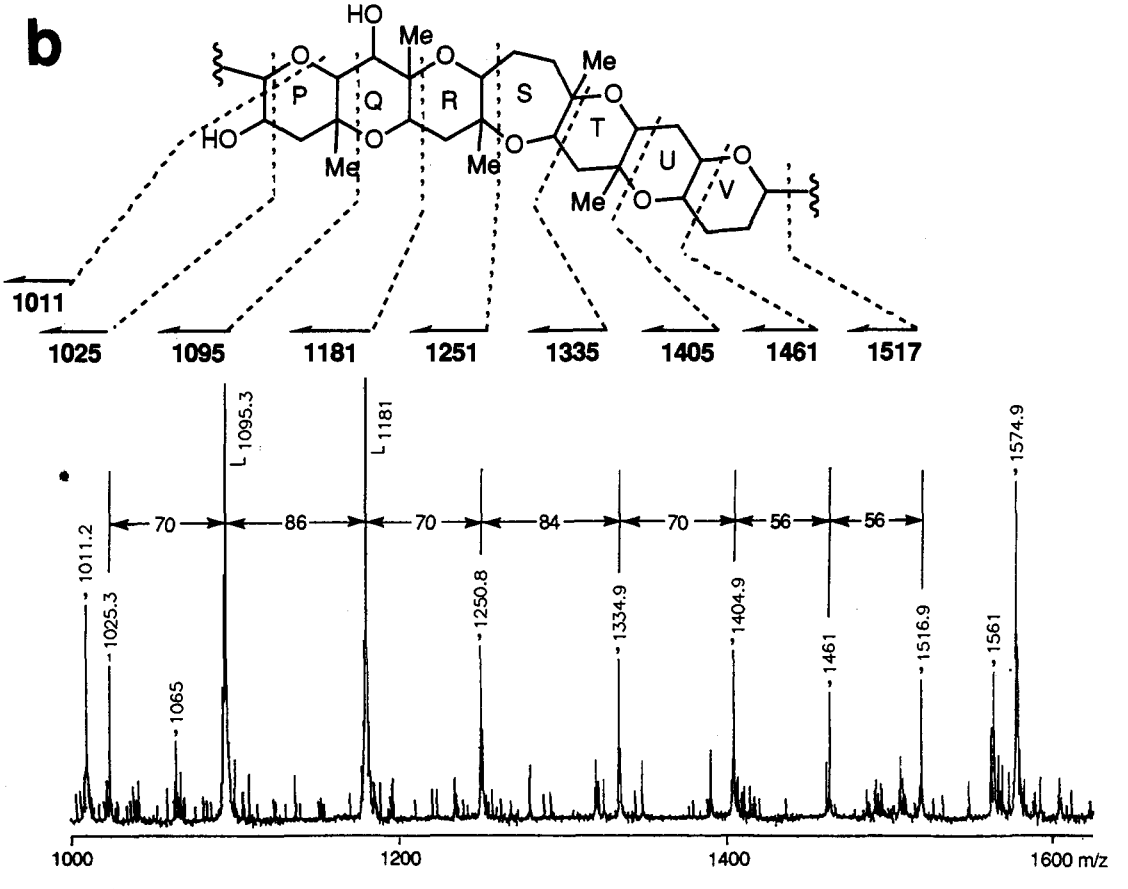
b
HO
Me
P
Q
R
S
T
U
V
1011
1025
1095
1181
1251
1335
1405
1461
1517
1095.3
1181
1574.9
70
86
70
84
70
56
56
1011.2
1025.3
1065
1250.8
1334.9
1404.9
1461
1516.9
1561
1000
1200
1400
1600 m/z

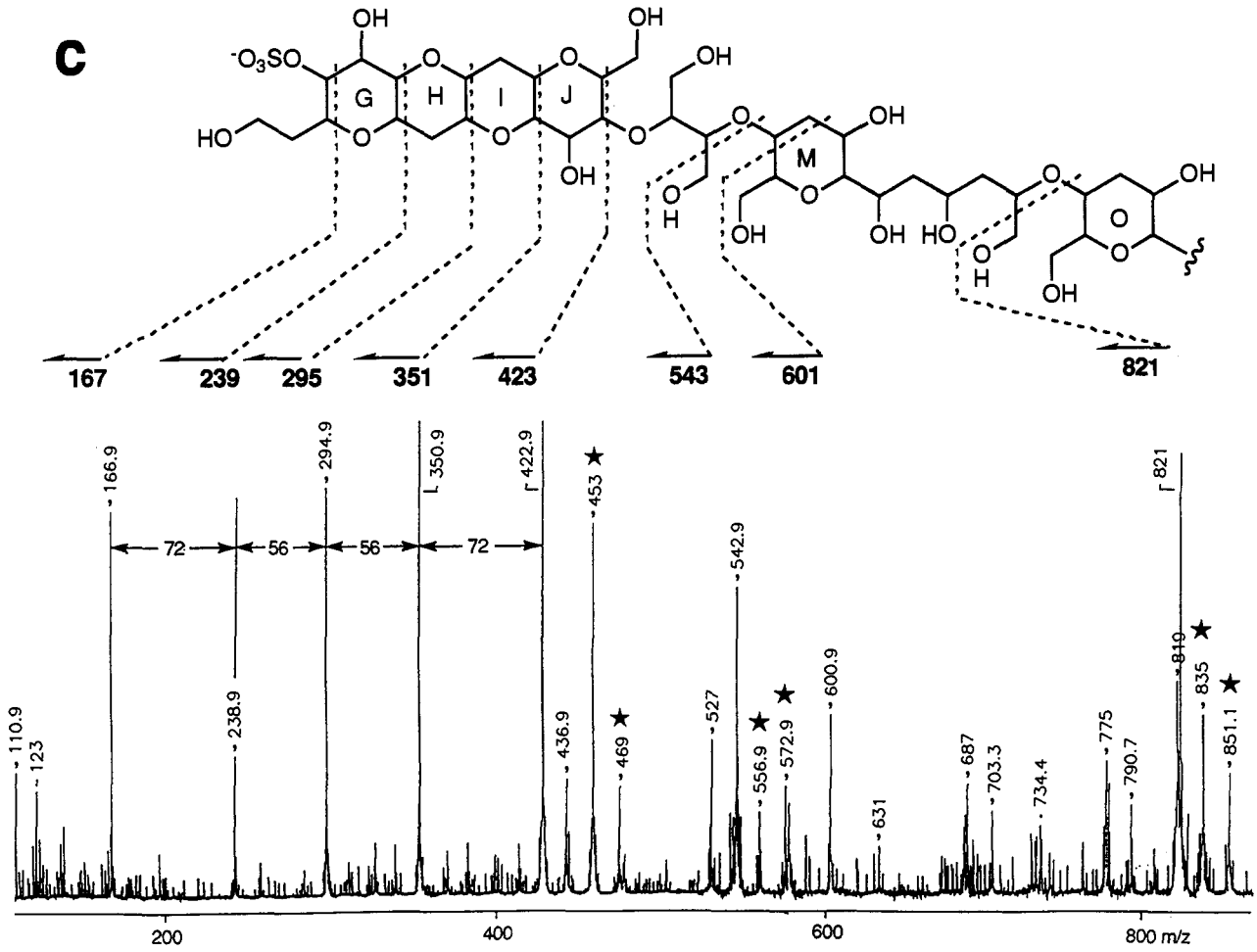

Figure 6. Negative ion FAB CAD MS/MS spectrum of fragment B (**3**). The spectrum was taken for the molecular related ion $(M-Na)^-$ at *m/z* 2305. It was shown in three parts: a was for the part of C100–C135, b for C76–C99, and c for C37–C75. Stars on ion peaks in c represent the bond breaks on both sides of acyclic ether bonds at C72/C68, C60/C56, and C55/C51.

the terminus of the molecule played an important role in simplifying the spectrum. A negative charge was localized at that position, thereby causing the fragment ions from that side of the molecule to appear in the spectrum.

As was the case with yessotoxin,[20] the CAD MS/MS of fragment B showed a series of prominent fragment ions generated by bond cleavage at the characteristic sites of ether rings, e.g. differences of 56 mass units (mu) observed between two consecutive peaks, like those in rings H, I, U, and A′, corresponded to C_3H_4O, indicating the presence of a 6-membered ether ring; a difference of 70 mu would indicate a 6-membered ring bearing a methyl (or a 7-membered ring), and 84 mu would correspond to a 7-membered ring plus a methyl (or to an 8-membered ring). Absence or presence of a methyl group on a cyclic ether could be determined by the NOESY and HMBC data as described above.

As depicted in Figure 6, the prominent ion peaks clearly indicated the sequence of cyclic ethers for rings G–J, P–V, and W–B′, but the presence of background peaks above m/z 2000 in the spectrum prevented unambiguous identification of peaks due to rings C′/D′, D′/E′, and E′/F′. However, the structure of this moiety was evident on the basis of the NMR data as seen in Figure 5. Mechanisms for the generation of some ions, those at *m/z* 1771.3 and 1673.5, are unknown, since they appeared to be derived from cleavage of three or more bonds followed by rearrangement.

The acyclic ethers produced as a result of the periodate degradation underwent fragmentation at either side of the ether linkages (starred ion peaks in Figure 6c), which allowed us to sequence the four parts C37–C53, C54–C57, C58–C69, and C70–C135. All these MS/MS data unambiguously supported structure **3**.

Reconstruction of the Entire Structure of Maitotoxin. There still remained some problems for the determination of the total structure after structures of fragments A, B, and C were secured. The first question to be answered was whether any portions besides fragment C were lost during degradation and purification. FABMS revealed the molecular weights of fragments A and B to be *m/z* 964 and 2328 (as sodium salts), respectively, and that of fragments C was surmised to be 142. Their sum (*m/z* 3434) was 11–13 mu greater than the molecular weight of MTX obtained by FABMS. As described above, at least six vicinal diol groups were cleaved by the $NaIO_4/NaBH_4$ reactions, with two protons being added at each cleavage site. When this is taken into account, the two sets of data—sum of the fragments versus intact MTX—agreed very well. Thus it was clearly demonstrated that no unknown fragments were lost during degradation.

The three fragments were then assembled into one piece on the basis of the TOCSY and DQF-COSY data of intact MTX (see the supplementary material for previous papers[1b]), which gave rise to cross peaks showing the connections of H35/H36/H37/H38 for fragments A/B and of H134/H135/H136/H137 for fragments B/C.

The next problems for total structural elucidation were how to reconstruct the vicinal diol moieties in MTX from pairs of the hydroxymethyl groups in the fragments and how to assign NMR signals due to those parts that had been affected by bond cleavage. A pair of hydroxymethyls at C16 and C17 was reconstructed to form ring A on the basis of the spin connectivities of C15–C18

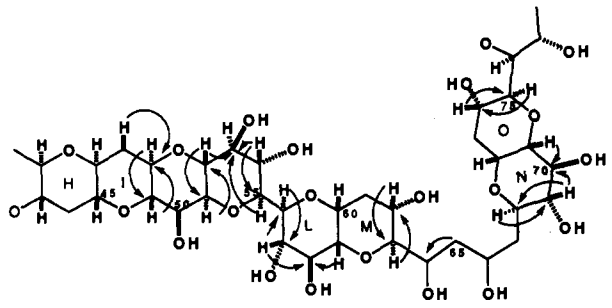

Figure 7. Interpretation of C-H TOCSY data for the central part of maitotoxin (**1**). Arrows denote the C–H TOCSY correlations between protons (a tail) and the neighboring carbons (a head). ^{13}C NMR chemical shifts in CD_3CN/D_2O (1:1) of the carbons are as follows: δ C48, 67.5; C49, 84.1; C50, 69.4; C51, 73.7; C52, 71.1; C53, 78.1; C54, 69.2; C55, 76.7; C56, 70.6; C57, 70.3; C58, 68.8; C59, 75.2; C60, 71.2; C61, 32.4; C62, 65.8; C63, 76.5; C64, 66.6; C68, 70.7; C69, 75.4; C70, 68.5; C71, 75.9; C72, 71.0; C73, 32.8; C74, 64.7; C75, 71.5 (see the supplementary material).

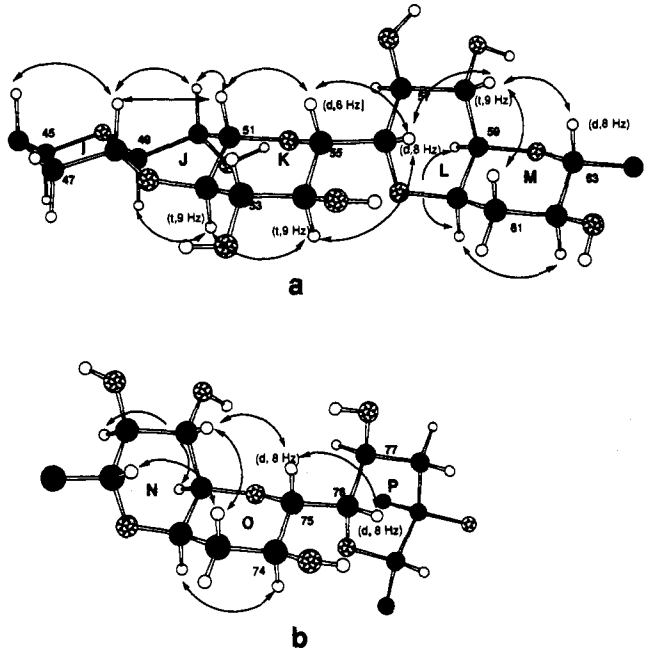

Figure 8. Stereostructures of rings H–M (a) and rings N–P (b) constructed by NOEs and coupling constants. Double-headed arrows indicate the NOEs mainly observed in the NOESY of **1**. In the parentheses are shown multiplicities of the ^1H signals (d, doublet; t, triplet) and coupling constants, which were estimated by cross peaks shown in the NOESY or the high-resolution COSY of **1** (modeling was carried out with use of MM2 data).

shown in the DQF-COSY of MTX. The other three pairs resided in the central part of fragment B, which encompassed 13 consecutive oxymethines from C48 to C60 with very close ^1H chemical shifts and a pair of cis-fused 1,6-dioxadecalins (rings L/M and N/O), causing heavily overlapping ^1H signals.

The structure for C48–C74 was determined partly by high-resolution COSY and by the C–H TOCSY spectra of MTX. Connectivities of H47–H52 and H53–H59 were revealed either by the COSY spectra (see the supplementary material) or by the NOE data (see Figure 8a). Vicinal couplings were detected as cross peaks in the C–H TOCSY for C48, C49, C51, C52, C53, C55, C56, C57, and C58 as depicted in Figure 7. Connections of the repeating segments C57–C62 and C69–C74 were made by combined use of the C–H TOCSY and NOESY data (Figures 7 and 8). On the strength of all the spectral information, the three vicinal diol groups that had been cleaved could be reconstructed, leading to the complete planar structure of MTX with a molecular formula of $C_{164}H_{256}O_{68}S_2Na_2$ (MW 3422 as a disodium salt). Complete ^1H NMR assignments of MTX are given in Table 2.

Stereochemistry of Fragments A and B. The stereochemistry of fragment A was deduced chiefly on the basis of ^1H NOE data. Trans and cisoid fusion of each ether ring in fragment A was evident from NOE data (Figure 3) as had been determined for other brevetoxin-type compounds.[3,21,22] The orientations of C20–OH, C30–OH, and C34–OH were assigned as β, β, and α, respectively, by NOE data (Figure 3).

Polycyclic ethers in three clusters of rings G–J, P–V, and W–F′ in fragment B were assigned to be trans-fused on the basis of NOE data (Figure 5). Six-membered rings G/H/I, P/Q/R, T/U/V, W/X, Z/A′, and C′/D′/E′/F′ appeared to be in chair conformations with 2,3- and 5,6-trans being equivalent to 2,6- and 3,5 cisoid ring fusion. In the two oxepane systems (rings S and Y) and the 4-oxocene (ring B′), trans and cisoid fusion was evident by NOEs between H90/Me152 and H86/Me153 of ring S, between H106/H111 and Me157/Me158[23] of ring Y, and between H116/H122 of ring B′. Further evidence comes from the 1,2-antiperiplanar orientation which is suggested by very weak (or absent) NOEs between Me152/H86 and Me153/H90; H106/Me157 and Me158/H111, H116/H117 and H121/H122.

The orientations of the sulfate and hydroxyl groups on rings G, P, Q, and W, as well as the stereochemistries of C39, C76 and C134, were determined by NOE data shown in Figure 5. The stereochemistries of the other parts (rings J/K, L/M, and N/O) could not be established from fragment B because the periodate degradation led to opening of rings K, L, and N and resulted in disappearance of some stereogenic centers (e.g., C53, C54, C57, C58, C69, or C70). Stereochemical assignments of these parts were, therefore, carried out with use of intact MTX.

Stereochemistry of Maitotoxin. Of the four vicinal diols cleaved by periodate, the stereochemistry of C16–OH/C17–OH was readily assigned to be equatorial/axial on the basis of prominent NOEs due to H16/H17, H17/H18, and H16/H18, as well as a small J-coupling of H17 (triplet, J = 2–3 Hz) characteristic of an equatorial proton. The orientation of the C14 substituent of ring A was determined to be equatorial by NOE between H15 and H19 (see the supplementary material for ref 1b).

The other three diols resided in the central part of the molecule, and hence, their stereostructures were difficult to assign. By extensive 2D NMR measurements and detailed examination of the 2D charts, we were able to obtain some information about interproton coupling and NOEs. These data were best explained by the configurations shown in Figure 8, in which rings L/M and N/O are cis-fused; the configurations were supported by strong NOEs between H58/H63 and H59/H60 or H70/H75 and H71/H72, together with weaker coupling values between H59/H60 or H71/H72 (Figure 8). The orientations of hydroxyl groups on these rings were also assigned with use of the NOEs and $^3J_{H,H}$ data. The NOESY data further suggested trans–transoid fusing of ring J by giving rise to cross peaks between H48 and H51 or between H49 and H52; if ring J were a cisoid-fused tetrahydropyran, these two sets of protons should take a 1,4-antiaxial orientation, being too distant to give NOEs. The sole stereostructure that satisfied these NOE conditions was a transoid ring fusion (Figure 8a).

Stereochemical correlations between the clusters of ether rings was another problem to be solved. Those between rings K and L, rings O and P, or rings V and W were deduced using NOE and $^3J_{H,H}$ data with the aid of molecular mechanics calculations (MM2).[24]

(21) Nagai, H.; Murata, M.; Torigoe, K.; Satake, M.; Yasumoto, T. *J. Org. Chem.* **1992**, *57*, 5448–545.

(22) Satake, M.; Murata, M.; Yasumoto, T. *J. Am. Chem. Soc.* **1993**, *115*, 361–362.

(23) While an NOE between Me157 and Me158 was not directly detected due to their close chemical shifts, a relayed NOE from Me159 via Me158 to Me157 in the NOESY of acetyl fragment B demonstrated that Me157 and Me158 were located well within the NOE range (3 Å).

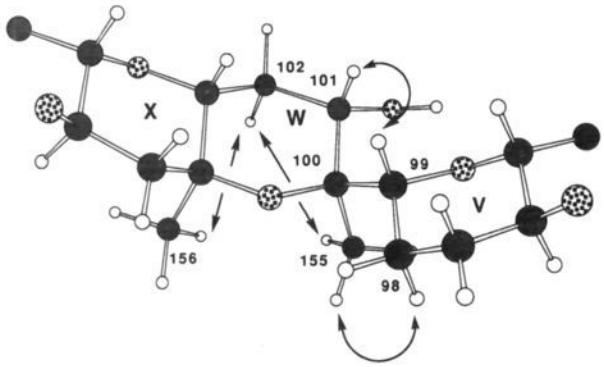

Figure 9. Stereostructure of rings V/W/X deduced by NOEs. Double-headed arrows indicate NOEs mainly observed between angular protons or methyls shown in the NOESY of **1**. This conformation represents the plausible rotamer with respect to the C99–C100 axis deduced by NOE data and MM2 calculations.

Rings K/L. Weak $^3J_{H,H}$ coupling and an intense NOE between H55 and H56 implied that an H55/H56 gauche rotamer was dominant around the C55–C56 axis as shown in Figure 8a. The present stereochemistry could better meet this condition, since the H55/H56 gauche was suggested to be the most preferable rotamer by MM2 calculations. On the other hand, if H56 had the alternative stereostructure (H56 was β in **1**), an antiperiplanar orientation of H55/H56 should be preferred by 2 kcal/mol over their gauche rotamer.

Rings O/P. There was no cross peak between H75/H76 in the DQF-COSY of MTX, while a prominent NOE was shown between them (Figure 8b). Thus these protons presumably are at a 90° angle with respect to the C75–C76 axis. MM2 calculations suggested that the present stereochemistry (H75 was α in **1**) with C74/C75 being *anti* to C76/C77 was preferable to that of the other possible conformer, in which C74 was gauche to C77. However, to satisfy the small value of $^3J_{H75/H76}$, the alternative configuration (H75 is β in **1**) would give rise to a C74/C77 gauche-like conformer about a C75/C76 axis; this was unlikely since its energy was higher than that of the ground-state conformation (C74/C77 and H75/H76 were antiperiplanar) by about 3 kcal/mol.

Rings V/W. Unlike the above cases, the stereochemical correlation between rings V and W could not be proven simply by NMR because of the very close ^{1}H chemical shifts of Me156 and Me155. Yet, an NOE was detected between Me155 and Hax102 (δ 1.58, quartet, J = 12 Hz, in CD_3CN/D_2O (1:1)[25] and the deshielded chemical shifts of Me155 and Me156 (δ 19.0 and 19.8) were typical for 2,6-diaxial dimethyls on tetrahydropyran, hence demonstrating equatorial substitution of C99 on ring W. As depicted in Figure 9, NOEs due to H99/H101 and Me155/H98 in the NOESY indicated antiperiplanar orientation of H99/Me155. MM2 calculations supported the present stereochemistry by giving a negative answer to the alternative configuration; in order to fulfill the NOE requirements, H99/Me155 should take an antiperiplanar orientation, which causes C98/C101 to be gauche. This conformation was energetically disfavored by more than 1.2 kcal/mol compared with the ground-state conformer, in which Me155 was gauche to H99. A rotamer similar to that in Figure 9 between two tetrahydropyran rings with an angular methyl was reported for thyrsiferol.[26]

The present study has disclosed the structure of MTX (**1**) with partial stereochemistry. Some stereogenic centers have been left unassigned (e.g., C5–C14, C36–C37, C64–C66, and C135–C139) because they are part of acyclic moieties. Stereoselective syntheses of the corresponding fragments will be necessary to determine these parts. The acyclic connections between ether rings, like those between rings K/L (C55/C56), O/P (C75/C76), and V/W (C99/C100), and their stereochemical correlations have been deduced on the basis of $^3J_{H,H}$ and/or NOEs, with the aid of MM2 calculations. Although the validity of rotation energy calculated by MM2 has generally become accepted, further spectroscopic evidence or syntheses of the corresponding parts will be necessary to confirm the present assignments.

The major difficulty in interpreting NMR data has been the severe overlapping of cross peaks in 2D spectra. In order to solve this problem, 3D NOESY-HMQC experiments were carried out[27] with use of a ^{13}C-enriched specimen. Preliminary results have suggested that these methods could be applicable to natural products with complicated large structures, if one can enrich a sample with ^{13}C nuclei; in the case of MTX, the abundance should be at least 5%. Greater separation of the NOESY signals in the 3D spectra will be of help in confirming the present structure.

One striking characteristic of structure **1** is the uneven distribution of polar functions; in addition to the two sulfate esters, 24 of a total of 28 hydroxyl groups reside in one half of the molecule (C1–C75), while only four hydroxyls are found in the other half (C76–C142). This structural feature causes amphiphilicity of MTX, which may play a role in exerting its extremely potent bioactivities. As mentioned earlier, Me155 and H99 are antiperiplanar with respect to a C99/C100 axis, which forces the hydrophobic part of the molecule (rings P–F′) to be nearly straight. These 17 polycycles are approximate 45 Å long, long enough to stretch across a biomembrane.

The pharmacological actions of MTX have been widely studied after its Ca^{2+} influx stimulation was reported by Ohizumi's group.[8,28] Recent papers have suggested that MTX activates non-voltage-sensitive Ca^{2+} channels like those operated by receptors.[29] Definitive experimental results that would account for the diverse actions of MTX have not appeared yet. We hope that our elucidation of the entire structure will stimulate further studies on the modes of action of this unique natural product.

From a biosynthetic point of view, MTX may well belong to the class of brevetoxin-type compounds as is the case with the other toxins produced by *G. toxicus* such as ciguatoxins or the gambieric acids.[21] Yet, there are some unprecedented features in the structure; e.g. the presence of two sets of cis-fused ether rings (rings L/M and N/O), transoid fusion of ring J, 2,2-connected bis(tetrahydropyrans) (rings O/P or rings V/W), absence of methyl substitution in C29–C78, or 13 contiguous oxygenated carbons (C48–C60). These characteristic features are mostly concentrated in the central part of the molecule. Biogenesis of this part might be different from that in the rest of the molecule, which is likely to be by "*polyepoxide cyclization*" as suggested for brevetoxins.[30] Together with the mechanism of producing an extremely long chain of 142 carbons, the biosynthesis of MTX will pose an exciting challenge.

Experimental Section

Chemicals. All solvents were purchased from standard vendors and used without further purification except for column chromatographies with MeOH and MeCN, which were distilled before use. Chemicals in

(24) Energy calculations of rotamers and ring conformations were carried out by molecular mechanics using Allinger's parameters: Werz, D. H.; Allinger, N. L. *Tetrahedron* **1979**, *35*, 3. Allinger, N. L. *J. Am. Chem. Soc.* **1977**, *99*, 8127.

(25) An axial proton at C102 was assigned on the basis of coupling constants determined by NOESY cross peaks versus Me156 or Me155 with a digital resolution of 1 Hz.

(26) Sakemi, S.; Higa, T.; Jefford, C. W.; Bernardinelli, G. *Tetrahedron Lett.* **1986**, *27*, 4287–4291.

(27) Satake, M.; Ishida, S.; Murata, M.; Yasumoto, T.; Utsumi, H.; Hinomoto, T. *Abstract of Papers in the 32nd NMR Conference*; Organizing Committee of the 32nd NMR Conference: Tokyo, 1993; 279–282.

(28) Kobayashi, M.; Ochi, R.; Ohizumi, Y. *Br. J. Pharmacol.* **1987**, *92*, 665.

(29) Soergel, D. G.; Yasumoto, T.; Daly, J. W.; Gusovsky, F. *Mol. Pharmacol.* **1992**, *41*, 487–493.

(30) (a) Nakanishi, K. *Toxicon* **1985**, *23*, 473. (b) Shimizu, Y. In *Natural Toxins*; Harris, J. B., Ed.; Clarendon Press: Oxford, U.K., 1986; pp 115–125.

the culture media of *Gambierdiscus toxicus* and for reactions including $NaIO_4$, $NaBH_4$, and Ac_2O were obtained from Wako Pure Chemicals. NMR solvents were obtained mostly from Aldrich Co. Ltd. with the best deuterium abundance available. CD_3OD was obtained partly from Merck and distilled before use.

Spectral Measurements. NMR Spectra of Fragments A and B. The ^1H–^1H COSYs of fragment A were recorded on a 400-MHz instrument (JEOL GSX-400) in three different solvents, CD_3OD, C_5D_5N, or $(CD_3)_2SO$. The COSY of the acetyl derivative of fragment A was measured on the same instrument in CD_3OD. ^1H–^1H COSY, TOCSY, NOESY, and DQF–COSY of fragment B were measured by a 600-MHz (AM-600, Bruker) or a 400-MHz (GSX-400) spectrometer in CD_3OD. Measurements of the ^1H–^1H COSY, TOCSY, and NOESY of an acetyl fragment B were carried out in CD_3OD with the same 600-MHz instrument.

NMR Spectra of MTX. The 1D and 2D ^1H NMR spectra of MTX were measured in three different solvent systems, CD_3OD/D_2O (19:1), CD_3CN/D_2O (1:1), or C_5D_5N/CD_3OD (1:1). For ^1H NMR measurements, 1–3 mM solutions of MTX were used depending on the solubility in the solvent systems. The ^1H–^1H COSY, NOESY, TOCSY, and DQF–COSY were recorded in all the three solvent systems either with a 600-MHz instrument (AM-600, Bruker) or with a 500-MHz instrument (AM-500, Bruker; GN-500, General Electric; and Omega 500, General Electric). The mixing time in NOESY experiments was usually 250 ms, and the spin-locking time in TOCSY was either 25 or 80 ms. A usual data size for 2D measurements was 2048 (t2) by 512 points (t1) with a phase sensitive mode except for those of COSY, and 2-fold zerofilling was carried out along the f1 axis to give 2D spectra with 2048 by 1024 point. For hetero 2D NMR, 10 mM MTX in CD_3OD/D_2O (1:1) or in C_5D_5N/CD_3OD (1:1) was used, corresponding to 20 mg in 600 μL. A solution of MTX above a concentration of 10 mM sometimes caused loss of resolution in the ^1H dimension. ^{13}C NMR and ^{13}C-observed ^1H–^{13}C COSY spectra were measured at 125 MHz with a GN-500 instrument in ^1H-decoupled modes. Inverse 2D experiments including HMQC, HMBC (optimized for 10 Hz), or 2D TOCSY-HMQC (spin-locking time of 20 ms) were determined at 500 MHz in CD_3CN/D_2O (1:1) by an Omega 500 instrument. 2D NOESY-HMQC (mixing time of 300 ms) and HMBC were measured also at 600 MHz (JMR A-600, JEOL, see the supplementary material).

Negative Ion FAB Mass Spectra of MTX. The FABMS of MTX was measured by a JMS HX-110 mass spectrometer (JEOL) at an accelerating voltage of 10 kV. The matrix was diethanolamine or a 1:1 mixture of glycerol and thioglycerol.[7] The negative ion FABMS of fragment A was recorded by a JMS DX-303 HF at 3 kV with use of glycerol as a matrix.

CAD MS/MS Spectra of Fragment B. The MS/MS spectra were measured in a negative ion FAB mode with a JMS HX-110/HX-110 tandem mass spectrometer (JEOL) with use of 2,2′-dithiodiethanol as a matrix at resolution of 2000. The geometry of the spectrometer was EBEB with an accelerating voltage of 10 kV equipped with a variable dispersion array detector (JOEL, MS-ADS11). A collision cell located in the third field-free region was floated at 8 kV. Helium was introduced to cause the dissociation at a pressure that reduced the intensity of precursor ions to 30%.

Culture of *Gambierdiscus toxicus* and Purification of Maitotoxin. As described in the previous paper,[6,7] *G. toxicus* was isolated from seaweeds from the Gambier Islands, French Polynesia. The clonal culture of the alga was established but it was not axenic. The culture (4000 L/year) for production of MTX was carried out in 3-L Fernbach flasks with 2 L of ES-1 medium[31] and kept at 25 °C for 37 days with 18 h/6 h of a light/dark cycle. The cell density reached (1–2) × 10^3 cells/mL when harvested. Extraction and purification of MTX were essentially the same as previously described.[7] The algal cells (ca. 2 × 10^9 cells in 1000 L of the culture media) were collected by filtration, and the retained cells on filter papers were extracted first with MeOH and then with $MeOH/H_2O$ (1:1) under reflux. The combined extracts were suspended in $MeOH/H_2O$ (8:2), defatted with CH_2Cl_2, and reextracted with 1-butanol. The extract was concentrated, loaded on a column of silica gel (Mallinckrodt, 32 × 120 mm), and eluted successively with $CHCl_3$/MeOH (7:3 and 1:1). The crude toxin in the last fraction was further purified by successive chromatography through a column of ODS (Fuji Gel Q3) eluted with a $MeOH/H_2O$ system and a column of C8 (Develosil, Nomura Chemicals) with $MeCN/H_2O$. The final purification was carried out by repeated HPLC (twice or three times) on a column of TMS (Develosil, 10 × 250 mm) eluted with aqueous 35% MeCN to furnish 4–5 mg of pure MTX from 1000 L of culture. During purification, location of MTX in the eluate of a column was determined either by mouse lethality tests (16–20-g male mice injected intraperitoneally with an aliquot of the suspended sample in 1% Tween 60 in H_2O) or by hemolytic tests using a 1% mouse blood cell suspension in saline.

Periodate Degradation and Purification of the Products. MTX (8.1 mg, 2.4 μmol) was treated with 30 μmol of $NaIO_4$ in 200 μL of H_2O for 10 min at room temperature. The products were then reduced with 70 μmol of $NaBH_4$ in 1 mL of MeOH for 10 min at room temperature. After addition of acetone (50 μL) and neutralization with 10% aqueous NH_4Cl, the organic solvents were removed from the reaction mixture and the residue was loaded on a Sep-pak C18 cartridge (Waters). After the cartridge was washed with 3 mL of H_2O, the products were eluted with 5 mL of MeOH. The MeOH fraction was separated by HPLC on a reversed-phase column of TMS (Rosil TMS, BioRad, 8 × 250 mm) using a linear gradient elution with MeCN in 5 mM potassium phosphate buffer at pH 6.5, starting from 60% MeCN at a rate of 0.5%/min with a flow rate of 1.0 mL/min. Throughout HPLC, fragment A was eluted first at 50 mL and fragment B was at 96 mL while no fragment C was recovered from HPLC. In order to remove the phosphate salts, the eluate was evaporated, suspended in H_2O, and loaded on the same C18 cartridge. After being washed with 5 mL of H_2O, the retained products were eluted with aqueous 95% MeOH (5 mL) and then MeOH (5 mL). Yields of fragments A and B were 70% and 92%.

Acknowledgment. This research was assisted by Messrs. A. Yokoyama, M. Sasaki, H. Ohmura, T. Kaneta, and K. Hokii and by Misses E. Iwama, N. Furuya, and A. Sato in isolating maitotoxin and in culturing the dinoflagellate. We are grateful to Dr. T. Iwashita, Suntory Institute, Dr. A. Ueno, Tohoku University, Dr. M. Oyabu, Shimadzu Co. Ltd., Dr. Wälchli, Japan Bruker, and Messrs. T. Hinomoto and H. Utsumi, JEOL Co. Ltd., for NMR measurements; to Prof. K. Tachibana, the University of Tokyo, for discussions; and to Prof. P. J. Scheuer, the University of Hawaii, for critical reading of the manuscript. The present study was supported in part by a grant-in-aid from the Ministry of Education, Science, and Culture, Japan, and by the Naito Foundation.

Supplementary Material Available: Figures showing ^1H–^1H COSYs of fragment A (**2**) with the assignments of cross peaks and its acetyl derivative and high-resolution COSY, C–H TOCSY with partial assignments, HMBC, and 2D NOESY-HMQC of of MTX (**1**) (9 pages). This material is contained in many libraries on microfiche, immediately follows this article in the microfilm version of the journal, and can be orderedfrom the ACS; see any current masthead page for ordering information. The other 2D NMR data are also available as supplementary material for the previous two communications.[1a,b]

(31) Provasoli, L. In *Proceedings of the U. S.-Japan Conference Held at Hakone*; Watanabe, A., Hattori, A., Eds.; *Japan Society of Plant Physiology*: Tokyo, 1966; pp 63–75.